# Miscibility and Interactions in Blends and Complexes of Poly(*N*-acryloyl-*N*′-phenylpiperazine) with Acidic Polymers

**S. H. Goh,* Y. Liu, and S. Y. Lee**

*Department of Chemistry, National University of Singapore, Singapore 119260, Republic of Singapore*

**C. H. A. Huan**

*Department of Physics, National University of Singapore, Singapore 119260, Republic of Singapore*

*Received August 6, 1999*

ABSTRACT: Poly(*N*-acryloyl-*N*′-phenylpiperazine) (PAPP) forms miscible blends with poly(*p*-vinylphenol) (PVPh), and it forms complexes with three stronger acidic polymers, namely, poly(styrenesulfonic acid) (PSSA), poly(vinylphosphonic acid) (PVPA), and poly(acrylic acid) (PAA). Fourier transform infrared spectroscopy and X-ray photoelectron spectroscopy were used to study the nature of interpolymer interactions in these blends and complexes. All three types of interacting sites of PAPP are involved in interactions with the acidic polymers. PAPP interacts with PVPh and PAA through hydrogen-bonding interaction, whereas it interacts with PSSA and PVPA through a combination of hydrogen-bonding and ionic interactions. As compared to poly(*N*-acryloyl-*N*′-methylpiperazine), the interactions between PAPP and the acidic polymers are less intense because of the steric shielding effect of the phenyl groups and the lower basicity of the tertiary amine nitrogen.

## Introduction

Two dissimilar polymers are likely to be miscible with each other if they possess functional groups that are capable of interacting with each other. Therefore, a proton-donating polymer is likely to be miscible with a proton-accepting polymer. Polymer blends are commonly prepared by solution blending in research laboratories. The two polymers are separately dissolved in a common solvent, and the two polymer solutions are then mixed. The polymer blend is obtained by either evaporating the solvent (solution casting) or precipitating the polymers in a nonsolvent (coprecipitation). In many cases, the mixing of the two polymer solutions leads to the formation of precipitates, which are commonly called interpolymer complexes or simply complexes.[1] The formation of complexes indicates that polymer−polymer interaction is stronger than polymer−solvent interaction, and the two polymers coprecipitate as highly associated materials. By increasing the number of interacting groups, a transition from immiscibility to miscibility and from miscibility to complexation can be achieved.[2−7]

However, the functional groups must be readily accessible to achieve miscibility.[8−10] If the functional groups become inaccessible due to factors such as intramolecular screening, steric shielding, or self-association, the miscibility behavior of the polymer blends can be significantly affected. For example, poly(2-vinylpyridine) is less readily miscible with other polymers as compared to poly(4-vinylpyridine) because its pyridine nitrogen atoms are less accessible for interaction.[11,12]

We have recently reported the miscibility and interactions in blends and complexes of poly(*N*-acrylolyl-*N*′-methylpiperazine) (PAMP) with several acidic polymers.[13,14] Each PAMP segment possesses three interacting sites: the carbonyl oxygen and the two nitrogen atoms. Using Fourier transform infrared (FTIR) spectroscopy and X-ray photoelectron spectroscopy (XPS), we have shown that all three interacting sites of PAMP are interacting with the acidic polymers. The present study deals with poly(*N*-acryloyl-*N*′-phenylpiperazine) (PAPP) in order to study the effect of the replacement of methyl groups of PAMP by phenyl groups on the miscibility and interactions with acidic polymers.

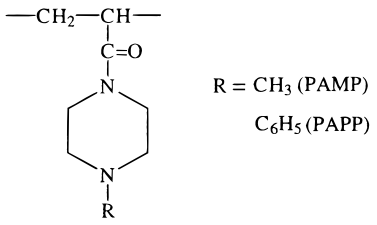


## Experimental Section

**Materials.** PAPP ($M_n$ = 28 000, $M_w$ = 44 000, glass-transition temperature ($T_g$) = 87 °C) was synthesized according to the procedures reported by Danusso et al.[15] Poly(*p*-vinylphenol) (PVPh) ($M_w$ = 22 000, $T_g$ = 154 °C), poly(styrenesulfonic acid) (PSSA) ($M_n$ = 22 500), and poly(vinylphosphonic acid) (PVPA) (molecular weight information not available, $T_g$ = 165 °C) were obtained from Polysciences, Inc. Poly(acrylic acid) (PAA) ($M_v$ = 450 000, $T_g$ = 127 °C) was supplied by Aldrich Chemical Co., Inc. The $T_g$ of PSSA was difficult to detect by differential scanning calorimetry (DSC).

**Preparation of Blends and Complexes.** Similar to the previous studies,[13,14] ethanol was used as the solvent for PVPh, and ethanol/water (1:1 v/v) was used as the solvent for PSSA, PVPA, and PAA because these polymers dissolved more readily in the mixed solvent than in ethanol. Polymer complexes were obtained by mixing appropriate amounts of ethanol/water solutions (1% w/v) of polyacid and PAPP. After 1 h of continuous stirring, polymer complexes in the form of precipitates were isolated by centrifugation and washed repeatedly with the mixed solvent. The complexes were then dried in vacuo at 90 °C for at least 2 weeks. The ratio of the amount of dried complex to the total amount of the two polymers in the initial solutions gives the yield of the complex. The bulk compositions of various complexes were calculated from their

10.1021/ma991320+ CCC: $18.00 
Published on Web 11/24/1999

**Table 1. Characteristics of PAPP/PVPh Blends**

| blend | 0.19APP0.81VP | 0.36APP0.64VP | 0.56APP0.44VP |
|---|---|---|---|
| bulk composition[a] | 0.30 | 0.50 | 0.70 |
| bulk composition[b] | 0.19 | 0.36 | 0.56 |
| surface composition[b] | 0.18 | 0.32 | 0.53 |
| $T_g$ (°C) | 140 | 133 | 116 |
| N (amide) 1s peaks (eV) | 399.7, 400.5 | 399.7, 400.5 | 399.7, 400.5 |
| N (amine) 1s peaks (eV) | 399.0, 400.0 | 399.0, 400.0 | 399.0, 400.0 |
| fraction of the high-BE peak of N (amide) 1s | 0.30 | 0.23 | 0.17 |
| fraction of the high-BE peak of N (amine) 1s | 0.16 | 0.18 | 0.16 |

[a] Weight fraction of PAPP. [b] Mole fraction of PAPP.

nitrogen contents as determined by elemental analysis using a Perkin-Elmer 2400 elemental analyzer.

The mixing of the ethanol solutions of PVPh and PAPP did not lead to precipitation. The mixed solution was allowed to evaporate to dryness. The cast blends were similarly dried in vacuo at 90 °C for 2 weeks. All of the dried blends and complexes were stored in a desiccator to prevent moisture absorption.

The surface compositions of the blends and complexes were determined by XPS based on the nitrogen/oxygen peak−area ratios after correction with appropriate sensitivity factors.

The PAPP/PVPh blends and PAPP/PSSA, PAPP/PVPA, and PAPP/PAA complexes are designated as *x*APP*y*VP, *x*APP*y*SSA, *x*APP*y*VPA, and *x*APP*y*AA, respectively, where *x* and *y* are the mole fractions of PAPP and the corresponding acidic polymer in the bulk of the blend or complex.

***T*g Measurements.** The glass-transition temperatures ($T_g$'s) of various samples were measured with a TA Instruments 2920 differential scanning calorimeter using a heating rate of 20 °C/min. Each sample was subjected to several heating/cooling cycles to obtain reproducible $T_g$ values. The initial onset of the change of slope in the DSC curve is taken to be the $T_g$.

**FTIR Characterization.** FTIR spectra were recorded on a Bio-Rad 165 FTIR spectrophotometer. Sixty-four scans were signal-averaged at a resolution of 2 $cm^{-1}$. Spectra were recorded at 150 °C using a SPECAC high-temperature cell, equipped with an automatic temperature controller, which was mounted in the spectrophotometer. Samples were prepared by grinding the dry blend or complex with KBr powder and compressing the mixture to form disks.

**XPS Measurements.** XPS measurements were made on a VG ESCALAB MKII spectrometer with a Mg Kα X-ray source (1253.6 eV photons). Various blends and complexes were ground to fine powders and then mounted on standard sample studs by means of double-sided adhesive tape. The X-ray source was run at 12 kV and 10 mA. The pressure in the analysis chamber was maintained at $10^{-8}$ mbar or lower during measurements. All core-level spectra were referenced to the C 1s neutral carbon peak at 284.6 eV and obtained at a takeoff angle of 75°. Each spectrum was curve-fitted using the XPSPEAK95 version 3.1 software. In the curve fitting, the widths (fwhm) of Gaussian peaks were maintained constant for all components in a particular spectrum.

## Results and Discussion

**General Characteristics of Blends and Complexes.** The mixing of the ethanol solutions of PVPh and PAPP did not lead to precipitation. All of the ethanol-cast PAPP/PVPh blends were transparent and each showed a single $T_g$, indicating miscibility. Some characteristics of the blends are shown in Table 1. As shown in Figure 1, the $T_g$ composition curve for the PAPP/PVPh blends can be fitted by the Kwei equation:[16,17]

$$T_g(\text{blend}) = [(w_1T_{g1} + kw_2T_{g2})/(w_1 + kw_2)] + qw_1w_2$$

where $k$ and $q$ are fitting constants and $w_i$ is the weight fraction of polymer $i$ in the blend. The curve in Figure 1 was drawn using $k$ and $q$ values of 1 and 50, respectively. The $T_g$ values of the blends show small positive deviations from the expected $T_g$ values based on a linear additivity rule. The positive deviations of the $T_g$ values of the PAPP/PVPh blends are smaller than those of the PAMP/PVPh blends.[13] The $k$ and $q$ values of the PAMP/PVPh blends are 1 and 180, respectively. If the $q$ values are taken to be a measurement of intermolecular interactions,[17] it follows that PVPh interacts more strongly with PAMP than it does with PAPP.

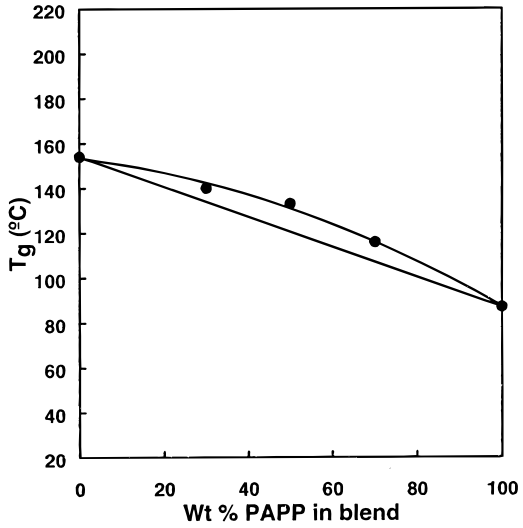


**Figure 1.** $T_g$ composition curve of PAPP/PVPh blends.

Besides a strong polymer−polymer interaction, the formation of complexes also requires the chain lengths of the interacting polymers to exceed a certain critical value.[18−20] A long polymer chain allows more cooperative interactions, thus facilitating complex formation. For example, we have found that PVPh forms complexes with a high-molecular-weight PAMP (PAMP−H, $M_w$ = 95 000) in ethanol but not with a low-molecular-weight PAMP (PAMP-L, $M_w$ = 3700).[13] Because the molecular weight of PAPP is lower than that of PAMP−H, the inability of PAPP to form complexes with PVPh might be due to its lower molecular weight. However, we have also found that poly(*N*-methyl-4-piperidyl methacrylate) ($M_w$ = 6000) and poly[2-(dimethylamino)ethyl methacrylate] ($M_w$ = 25 800) form complexes with PVPh in ethanol.[21,22] It appears that the molecular weight of PAPP is sufficiently high to meet the critical chain length requirement to form complexes. Moreover, as will be discussed later, the interaction between PAPP and PVPh is weaker than that between PAMP and PVPh. Therefore, the inability of PAPP to form complexes with PVPh is due more to the weaker intermolecular interaction rather than the chain length effect.

On the other hand, PAPP formed interpolymer complexes with PSSA, PVPA, and PAA in ethanol/water (1:

**Table 2. Characteristics of PAPP/PSSA Complexes**

| complex | 0.29APP0.71SSA | 0.40APP0.60SSA | 0.36APP0.64SSA |
|---|---|---|---|
| feed composition[a] | 0.27 | 0.46 | 0.67 |
| bulk composition[a] | 0.29 | 0.40 | 0.36 |
| surface composition[a] | 0.27 | 0.34 | 0.33 |
| yield (wt %) | 61 | 87 | 66 |
| N (amide) 1s peaks (eV) | 399.7, 400.5 | 399.7, 400.5 | 399.7, 400.5 |
| N (amine) 1s peaks (eV) | 399.0, 401.6 | 399.0, 401.6 | 399.0, 401.6 |
| fraction of the high-BE peak of N (amide) 1s | 0.14 | 0.32 | 0.16 |
| fraction of the high-BE peak of N (amine) 1s | 0.34 | 0.55 | 0.49 |

[a] Mole fraction of PAPP.

**Table 3. Characteristics of PAPP/PVPA Complexes**

| complex | 0.24APP0.76VPA | 0.35APP0.65VPA | 0.30APP0.70VPA |
|---|---|---|---|
| feed composition[a] | 0.18 | 0.33 | 0.54 |
| bulk composition[a] | 0.24 | 0.35 | 0.30 |
| surface composition[a] | 0.29 | 0.37 | 0.31 |
| yield (wt %) | 57 | 71 | 59 |
| N (amide) 1s peaks (eV) | 399.7, 400.5 | 399.7, 400.5 | 399.7, 400.5 |
| N (amine) 1s peaks (eV) | 399.0, 401.6 | 399.0, 401.6 | 399.0, 401.6 |
| fraction of the high-BE peak of N (amide) 1s | 0.11 | 0.22 | 0.16 |
| fraction of the high-BE peak of N (amine) 1s | 0.18 | 0.30 | 0.22 |

[a] Mole fraction of PAPP.

**Table 4. Characteristics of PAPP/PAA Complexes**

| complex | 0.22APP0.78AA | 0.27APP0.73AA | 0.33APP0.67AA |
|---|---|---|---|
| feed composition[a] | 0.13 | 0.25 | 0.44 |
| bulk composition[a] | 0.22 | 0.27 | 0.33 |
| surface composition[a] | 0.23 | 0.30 | 0.33 |
| $T_g$ (°C) (experimental) | 143 | 154 | 149 |
| $T_g$ (°C) (calculated) | 109 | 106 | 103 |
| yield (wt %) | 28 | 41 | 29 |
| N (amide) 1s peaks (eV) | 399.7, 400.5 | 399.7, 400.5 | 399.7, 400.5 |
| N (amine) 1s peaks (eV) | 399.0, 400.1 | 399.0, 401.1 | 399.0, 401.1 |
| fraction of the high-BE peak of N (amide) 1s | 0.13 | 0.21 | 0.11 |
| fraction of the high-BE peak of N (amine) 1s | 0.17 | 0.29 | 0.21 |

[a] Mole fraction of PAPP.

1) solutions. Tables 2−4 show the characteristics of various complexes. The surface composition and the bulk composition of the complex are quite close to each other, indicating that the surface energies of the component polymers are about the same. No distinct $T_g$ could be detected for the PAPP/PSSA and PAPP/PVPA complexes due to the inability to detect the $T_g$ of PSSA and the small heat capacity change upon glass transition of PVPA.

Only one glass-transition temperature was observed for each PAPP/PAA complex. As shown in Table 4, the $T_g$ values of the complexes are higher than those calculated from the linear additivity rule. Similarly, the PAPP/PAA complexes show smaller positive deviations in their $T_g$ values than those of the PAMP/PAA complexes.[14] Once again, this result may be taken to indicate that PAA interacts more strongly with PAMP than with PAPP.

The yields of the complexes are in the order PAPP/PSSA > PAPP/PVPA > PAPP/PAA. A similar trend was also observed for the PAMP complexes.[14] The more acidic the polymer, the higher is the yield. However, the yield of the PAPP complex is lower than that of the corresponding PAMP complex. As mentioned earlier, complexation is favored by a strong intermolecular interaction and a long polymer chain. Thus, the lower yield of the PAPP complex also indicates a weaker interaction in the PAPP complex than in the PAMP complex.

**FTIR Characterization.** The FTIR spectra in the carbonyl region for PAPP and its blends with PVPh are shown in Figure 2. Similar to PAMP, PAPP has a strong carbonyl stretching absorption band at 1640 $cm^{-1}$. The presence of a new band at 1653 $cm^{-1}$ in the PAPP/PVPh blends can be noted, indicating that the hydroxyl group of PVPh interacts with the lone-pair electrons on the nitrogen atom of the amide group through hydrogen bonding.[23,24] As the PVPh content in the blend de-

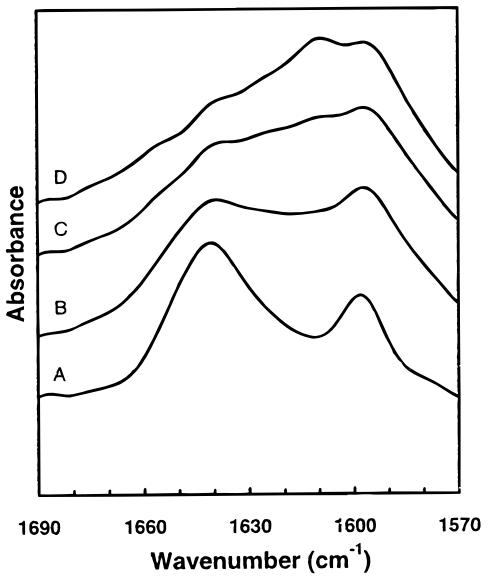


**Figure 2.** FTIR spectra, recorded at 150 °C, of the carbonyl region of PAPP and PAPP/PVPh blends: (A) PAPP, (B) 0.56APP0.44VP, (C) 0.36APP0.64VP, and (D) 0.19APP0.81VP.

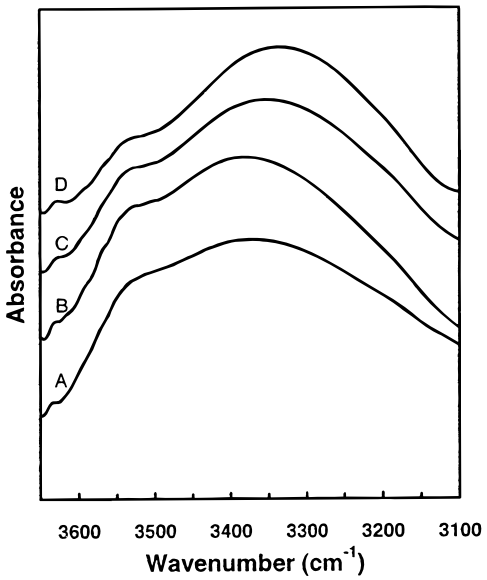


**Figure 3.** FTIR spectra, recorded at 150 °C, of the hydroxyl region of PAPP/PVPh complexes: (A) PVPh, (B) 0.19APP0.81VP, (C) 0.36APP0.64VP, and (D) 0.56APP0.44VP.

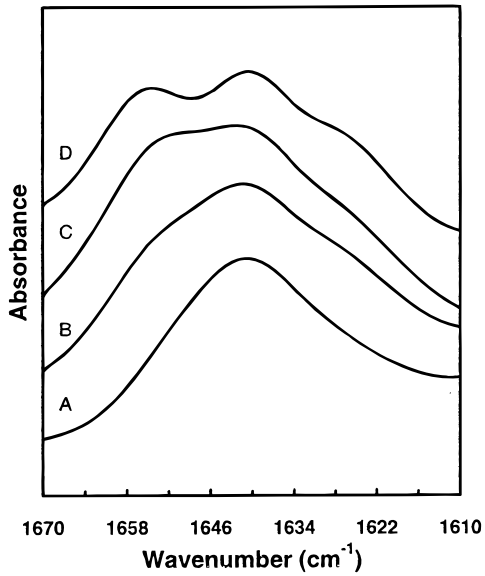


**Figure 4.** FTIR spectra, recorded at 150 °C, of the carbonyl region of PAPP and PAPP/PSSA complexes: (A) PAPP, (B) 0.40APP0.60SSA, (C) 0.36APP0.64SSA, and (D) 0.29APP0.71SSA.

creases, the intensity of this new band decreases. On the other hand, there is another new band located at 1625 $cm^{-1}$, showing the presence of hydrogen-bonding interaction between the hydroxyl group of PVPh and the carbonyl oxygen of PAPP. However, this peak is not distinct because of the interference of the benzene ring stretching band. It is concluded that the hydroxyl groups of PVPh interact with both hydrogen-bond interacting sites in the amide groups of PAPP.

However, the 1653 and 1625 $cm^{-1}$ bands of the PAPP/PVPh blends are weaker than those of the PAMP/PVPh blends.[13] The results indicate that the phenyl groups in PAPP hinder the interactions between the hydroxyl groups of PVPh and the carbonyl oxygens and the amide nitrogens of PAPP.

Figure 3 shows the infrared spectra of the PAPP/PVPh blends in the hydroxyl region at 150 °C. PVPh has a band centered at 3525 $cm^{-1}$ attributed to free hydroxyl groups and a broad band centered at 3369 $cm^{-1}$, which represents a broad distribution of self-associated hydroxyl groups. The center of the broad hydrogen-bonded hydroxyl band of the blend shifts from 3369 to 3340 $cm^{-1}$, showing that the intermolecular hydrogen-bonding interactions are stronger than the self-association of PVPh. The intensity of the free hydroxyl band at 3525 $cm^{-1}$ of the blends is reduced, indicating that more hydroxyl groups are involved in intermolecular interaction with PAPP. However, the reduction in the intensity of the free hydroxyl band is less pronounced as compared to that in the PAMP/PVPh blends.[13] Once again, the results demonstrate that the interaction between the hydroxyl groups of PVPh and PAPP is reduced by the presence of the phenyl groups.

Figure 4 shows the FTIR spectra in the carbonyl stretching region of PAPP and its complexes with PSSA. All of the complexes show the development of two new carbonyl bands at 1626 and 1655 $cm^{-1}$, in addition to the carbonyl band at 1640 $cm^{-1}$. These two new bands are more intense than those in the PAPP/PVPh blends, indicating a stronger interaction between PAPP and PSSA. However, the intensity of these two bands is less than that in the PAMP/PSSA complexes.[14]

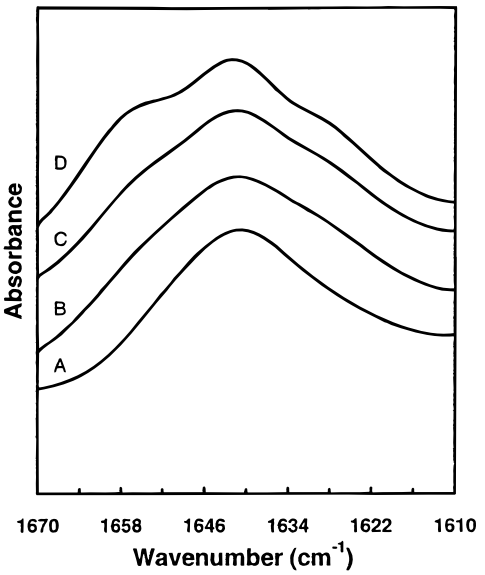


**Figure 5.** FTIR spectra, recorded at 150 °C, of the carbonyl region of PAPP and PAPP/PVPA complexes: (A) PAPP, (B) 0.35APP0.65VPA, (C) 0.30APP0.70VPA, and (D) 0.24APP0.76VPA.

Figure 5 shows the carbonyl region FTIR spectra of PAPP/PVPA complexes. The appearance of two new bands at 1654 and 1629 $cm^{-1}$ is noted. The intensity of the two bands is lower than that of the PAMP/PVPA complexes.[14] Therefore, PVPA also interacts with both the hydrogen-bond acceptor sites in the amide group of PAPP.

Figure 6 shows the FTIR spectra of the carbonyl group in PAPP/PAA complexes. The 1655 and 1627 $cm^{-1}$ bands are not distinct except for the complex with a high PAA content. From the intensity of the two new carbonyl bands, we can deduce that the intensity of interaction between PAPP and the acidic polymer decreases in the order PSSA > PVPA > PAA ≈ PVPh.

**XPS Characterization.** Figure 7 shows the N 1s spectra of PAPP and the three PAPP/PVPh blends. Similar to PAMP, the N 1s peak of PAPP can be

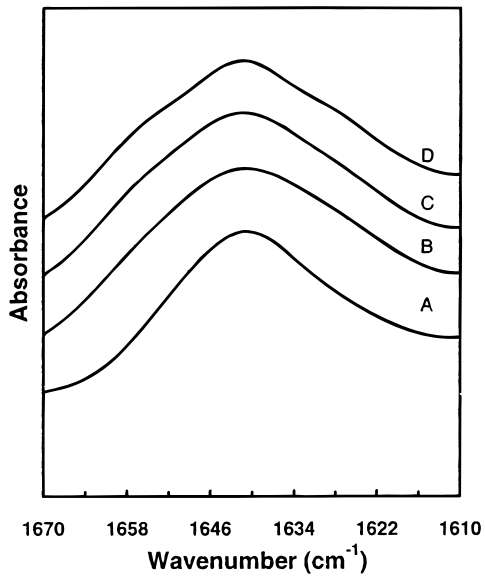


**Figure 6.** FTIR spectra, recorded at 150 °C, of the carbonyl region of PAPP and PAPP/PAA complexes: (A) PAPP, (B) 0.33APP0.67AA, (C) 0.27APP0.73AA, and (D) 0.22APP0.78AA.

deconvoluted into two component peaks: the amine N 1s peak at 399.0 eV and the amide N 1s peak at 399.7 eV. The N 1s peaks of the blends are broader and asymmetric, and each peak can be deconvoluted into four component peaks, with two remaining at 399.0 and 399.7 eV. The presence of two additional high-binding-energy (BE) N 1s peaks is evidenced in the spectra of all the blends, indicating that both types of nitrogen in PAPP interact with PVPh. The peak deconvolution is based on the principle that the sum of the two amine peaks equal to the sum of the two amide peaks. In all cases, the sum of the components peaks is in good agreement to the experimental signal. The BE values of the two high-BE N 1s peaks are 400.0 and 400.5 eV. The former peak, with a BE value 1.0 eV higher than 399.0 eV, arises from the interaction between the tertiary amine nitrogen and the hydroxyl group of PVPh. The BE value of the latter peak is 0.8 eV higher than 399.7 eV, and it arises from the interaction involving the amide nitrogen. The tertiary amine nitrogen interacts more strongly with PVPh than the amide nitrogen does, because the tertiary amine nitrogen shows a larger BE shift. The BE shift is indicative of the nature of interaction. A shift of about 1 eV indicates hydrogen-bonding interaction, whereas a shift of about 2−2.5 eV indicates ionic interaction.[25−27] The BE shifts of the PAPP/PVPh blends also show that the interaction between PAPP and PVPh is hydrogen-bonding.

The fractions of amine nitrogen and amide nitrogen of PAPP involved in hydrogen-bonding interactions can be estimated from the area of the high-BE N 1s peaks (Table 1). As compared to the PAMP/PVPh blends, the fractions of interacting amine and amide nitrogens are significantly smaller, particularly for the amine nitrogen. The XPS results show quantitatively that the presence of the phenyl groups in PAPP reduces its ability to interact with PVPh, and the effect is more pronounced for the amine nitrogen.

The N 1s spectra of PAPP and the three PAPP/PSSA complexes are shown in Figure 8. The complexation between PAPP and PSSA produces a distinct splitting of the N 1s peak into four components: two low-BE components at 399.0 and 399.7 eV and two new high-BE components at 400.5 and 401.6 eV. Therefore, both types of nitrogen in PAPP interact with PSSA. The

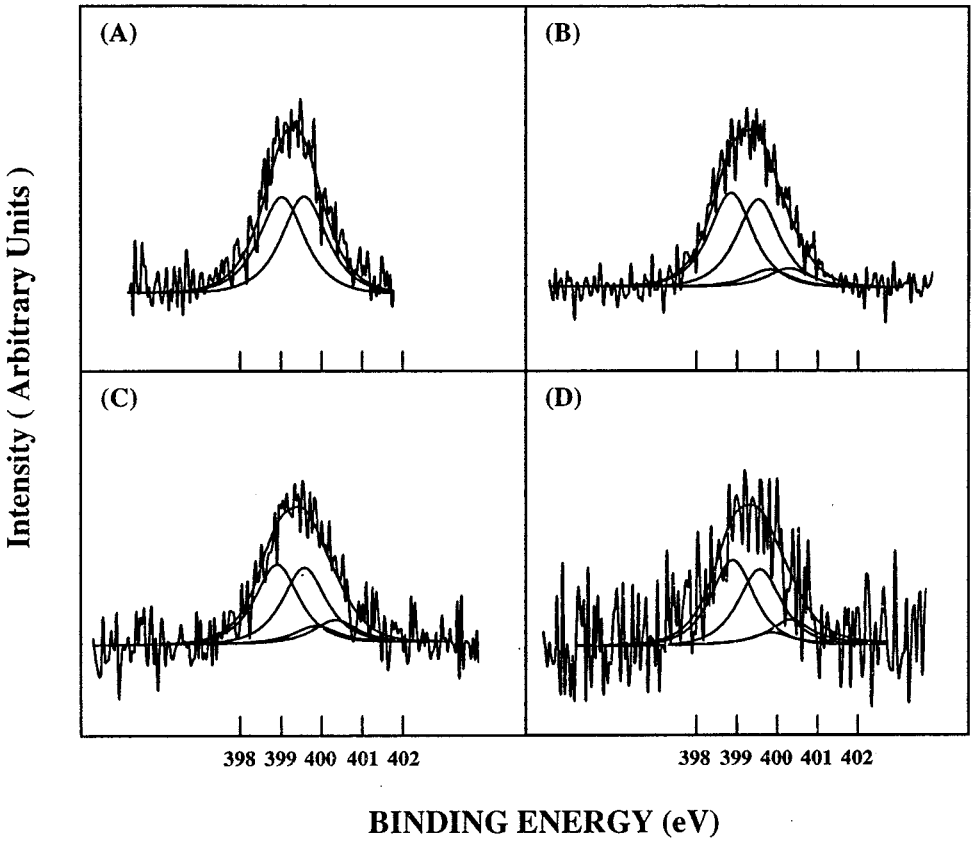


**Figure 7.** N 1s spectra of PAPP/PVPh blends: (A) PAPP, (B) 0.56APP0.44VP, (C) 0.36APP0.64VP, and (D) 0.19APP0.81VP.

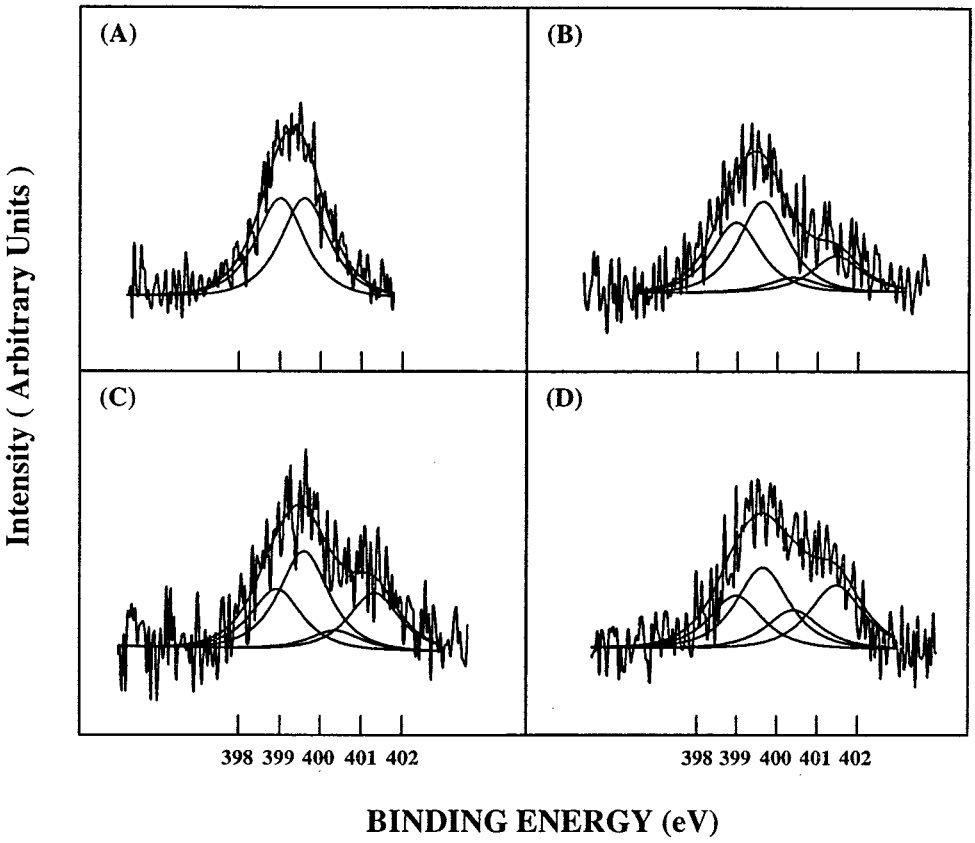


**Figure 8.** N 1s spectra of PAPP and PAPP/PSSA complexes: (A) PAPP, (B) 0.29APP0.71SSA, (C) 0.36APP0.64SSA, and (D) 0.40APP0.60SSA.

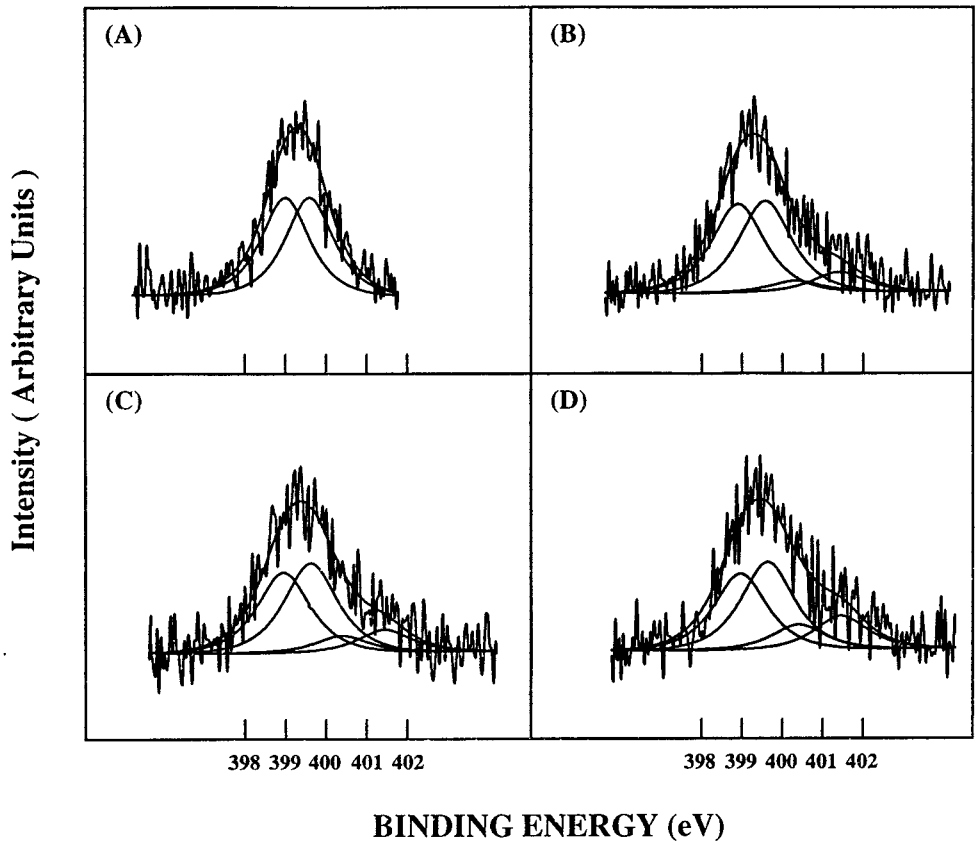


**Figure 9.** N 1s spectra of PAPP and PAPP/PVPA complexes: (A) PAPP, (B) 0.24APP0.76VPA, (C) 0.30APP0.70VPA, and (D) 0.35APP0.65VPA.

amide N 1s peak also shows a BE shift of 0.8 eV, showing that the amide nitrogen is involved in hydrogen-bonding interaction. On the other hand, the amine N 1s peak shows a BE shift of 2.6 eV, showing that the

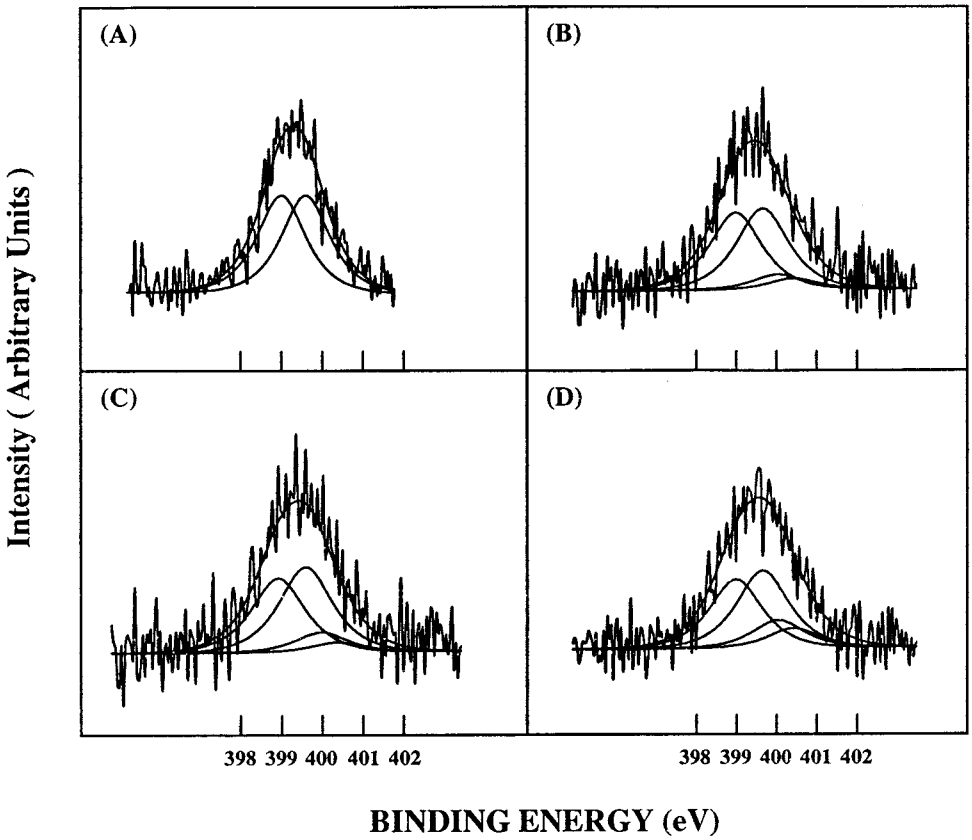


**Figure 10.** N 1s spectra of PAPP and PAPP/PAA complexes: (A) PAPP, (B) 0.22APP0.78AA, (C) 0.33APP0.67AA, and (D) 0.27APP0.73AA.

nitrogen is protonated by PSSA. The extent of protonation can also be calculated from the areas of the deconvoluted peaks, and the results are shown in Table 2. A substantial fraction of amine nitrogen is protonated. Therefore, in addition to hydrogen-bonding interaction, there is also ionic interaction between the protonated nitrogen and the sulfonate ion. Because ionic interaction is stronger than hydrogen-bonding interaction, PAPP interacts more strongly with PSSA than with PVPh.

Figure 9 shows the N 1s spectra of PAPP/PVPA complexes. Similarly, the amide N 1s peaks at 399.7 eV in all the three complexes show BE shifts of about 0.9 eV, indicating hydrogen-bonding interaction. On the other hand, the amine N 1s peaks at 399.0 eV show BE shifts of 2.6 eV, showing the presence of ionic interactions in all of the complexes. However, the fraction of protonation of the amine nitrogens is not as large as that in the PAPP/PSSA complexes because phosphonic acid is a weaker acid than sulfonic acid.

Figure 10 shows the N 1s spectra of PAPP/PAA complexes. The amide N 1s peaks at 399.7 eV in all three complexes show BE shifts of about 0.8 eV, indicating hydrogen-bonding interaction. The amine N 1s peaks at 399.0 eV show BE shifts of around 1.1 eV, indicating that the amine nitrogens are not protonated. It is interesting to note that some of the amine nitrogens in the PAMP/PAA complexes are protonated as evidenced by a BE shift of 2.1 eV.[14] Aromatic amines are much weaker bases than aliphatic amines. Therefore, the replacement of the methyl groups in PAMP by the phenyl groups not only introduces a steric shielding effect but also reduces the basicity of the amine nitrogen. Although PSSA and PVPA are still strong enough to protonate PAPP, the weaker acid PAA is unable to do so. As a result, PAA interacts with PAPP through hydrogen-bonding interaction only.

## Conclusions

PAPP is miscible with PVPh, whereas it forms complexes with PSSA, PVPA, and PAA. FTIR and XPS confirm that all the three types of interacting sites of PAPP are involved in interactions with the acidic polymers. XPS also shows that some of the amine nitrogens of PAPP are protonated by PSSA and PVPA. Therefore, hydrogen-bonding interaction exists between PAPP and PVPh or PAA, and a combination of hydrogen-bonding and ionic interactions exists between PAPP and PSSA or PVPA. Because of the steric shielding of the phenyl groups and the reduction of the basicity of the amine nitrogen, PAPP interacts less strongly with the acidic polymers as compared to PAMP.

**Acknowledgment.** The authors thank the National University of Singapore for its financial support of this research.

## References and Notes

(1) For a recent review on interpolymer complexation see: Jiang, M.; Li, M.; Xiang, M.; Zhou, H. *Adv. Polym. Sci.* **1999**, *146*, 121.
(2) Goh, S. H.; Lau, W. W. Y.; Lee, C. S. *Polym. Bull.* **1992**, *29*, 521.
(3) Zhou, H.; Xiang, M.; Chen, W.; Jiang, M. *Macromol. Chem. Phys.* **1997**, *198*, 809.
(4) Zhu, L.; Jiang, M.; Liu, L.; Zhou, H.; Fan, L.; Zhang, Y.; Zhang, Y. B.; Wu, C. *J. Macromol. Sci., Phys.* **1998**, *B37*, 805.
(5) Zhu, L.; Jiang, M.; Liu, L.; Zhou, H.; Fan, L.; Zhang, Y. *J. Macromol. Sci., Phys.* **1998**, *B37*, 827.
(6) Prinos, A.; Dompros, A.; Panayiotou, C. *Polymer* **1998**, *39*, 3011.

(7) Lu, S.; Pearce, E. M.; Kwei, T. K. *Polym. Adv. Technol.* **1996**, *7*, 553.
(8) Coleman, M. M.; Pehlert, G. J.; Painter, P. C. *Macromolecules* **1996**, *29*, 6820.
(9) Pehlert, G. J.; Painter, P. C.; Veytsman, B.; Coleman, M. M. *Macromolecules* **1997**, *30*, 3671.
(10) Pehlert, G. J.; Painter, P. C.; Coleman, M. M. *Macromolecules* **1998**, *31*, 8423.
(11) Zhou, X.; Goh, S. H.; Lee, S. Y.; Tan, K. L. *Polymer* **1997**, *38*, 5333.
(12) Velada, J. C.; Cesteros, L. C.; Katime, I. *Appl. Spectrosc.* **1996**, *50*, 893.
(13) Liu, Y.; Goh, S. H.; Lee, S. Y.; Huan, C. H. A. *Macromolecules* **1999**, *32*, 2, 1967.
(14) Liu, Y.; Goh, S. H.; Lee, S. Y.; Huan, C. H. A. *J. Polym. Sci., Part B: Polym. Phys.*, submitted for publication.
(15) Danusso, F.; Tanzi, M. C.; Levi, M.; Martini, A. *Polymer* **1990**, *31*, 1577.
(16) Kwei, T. K. *J. Polym. Sci., Polym. Lett. Ed.* **1984**, *22*, 307.
(17) Pennachia, J. R.; Pearce, E. M.; Kwei, T. K.; Bulkin, B. J.; Chen, J. P. *Macromolecules* **1986**, *19*, 973.
(18) Tsuchida, E.; Osada, Y.; Ohno, H. *J. Macromol. Sci., Phys.* **1980**, *B17*, 683.
(19) Bekturov, E. A.; Bimendina, L. A. *Adv. Polym. Sci.* **1981**, *41*, 99.
(20) Garary, M. T.; Ilamas, M. C.; Iglesias, E. *Polymer* **1997**, *38*, 5091.
(21) Luo, X. F.; Goh, S. H.; Lee, S. Y. *Macromolecules* **1997**, *30*, 4934.
(22) Huang, X. D.; Goh, S. H.; Lee, S. Y.; Zhao, Z. D.; Wong, M. W.; Huan, C. H. A. *Macromolecules* **1999**, *32*, 4327.
(23) Schmulbach, C. D.; Drago, R. S. *J. Phys. Chem.* **1960**, *64*, 1956.
(24) Bull, W. E.; Madan, S. K.; Willis, J. E. *Inorg. Chem.* **1963**, *2*, 303.
(25) Zhou, X.; Goh, S. H.; Lee, S. Y.; Tan, K. L. *Appl. Surf. Sci.* **1997**, *119*, 60.
(26) Zhou, X.; Goh, S. H.; Lee, S. Y.; Tan, K. L. *Appl. Surf. Sci.* **1998**, *126*, 141.
(27) Zhou, X.; Goh, S. H.; Lee, S. Y.; Tan, K. L. *Polymer* **1998**, *39*, 3631.

MA991320+